Graz University of Technology

MASTER THESIS

Investigation of the influence of the tunnel lining on the displacement development

Dominik Lebschy, Bsc

Institute for Rock Mechanics and Tunnelling
Graz University of Technology

Reviewer:

O.Univ.-Prof. Dipl.-Ing. Dr.mont. Wulf Schubert
Institute for Rock Mechanics and Tunnelling
Graz University of Technology

Graz, September 2014

Eidesstattliche Erklärung

Ich erkläre an Eides statt, dass ich die vorliegende Arbeit selbstständig verfasst, andere als die angegebenen Quellen/Hilfsmittel nicht benutzt und die den benutzten Quellen wörtlich und inhaltlich entnommene Stellen als solche kenntlich gemacht habe.

Graz, September 2014

Dominik Lebschy

Statutory Declaration

I declare that I have authored this thesis independently, that I have not used other than the declared sources / resources, and that I have explicitly marked all material which has been quoted either literally or by content from the used sources.

Graz, September 2014

Dominik Lebschy

Danksagung

An dieser Stelle möchte ich mich bei all jenen bedanken, die mich während meiner Studienzeit und im speziellen beim Verfassen dieser Masterarbeit unterstützt haben.

Für die ausgezeichnete Betreuung dieser Arbeit und die konstruktiven Diskussionen bedanke ich mich bei Herrn O.Univ.-Prof. Dipl.-Ing. Dr.mont. Wulf Schubert, Leiter des Institus für Felsmechanik und Tunnelbau. Ebenso bedanke ich mich bei Herrn Dipl.-Ing. Alexander Kluckner für die Hilfe und Unterstützung bei allen computertechnischen Problemen.

Bedanken möchte ich mich bei all meinen Freunden und Kollegen des Stahlbauzeichensaals für die gemeinsame Zeit und die vielen fröhlichen Stunden.

Danken möchte ich meiner Freundin Carina für die Unterstützung und die manchmal dringend benötigte Motivation.

Besonderer Dank gebührt meiner ganzen Familie, insbesonderes meinem Bruder Sebastian und meinen Eltern Paula und Siegfried für die Möglichkeit dieses Studium durchzuführen, die damit verbundene Unterstützung und den Rückhalt in jeder Lebenslage.

DANKE!

Abstract

One of the important factors for a succesfull and economic tunnel project is to realistically assess the displacement development in the excavated areas, to allow estimating the needed amount of over-excavation. One of the factors guiding the tunnel displacements is the interaction between the rock mass and the installed tunnel support. The development of a reliable displacement prediction method to a certain extend relies on the correct prediction of the influence of the support.
A series of 3-dimensional numerical simulations for both supported and unsupported tunnels was carried out to investigate the influence of the tunnel lining on the displacement development.
The simulation results were compared with existing analytical functions. With varrying input parameters the effect of different rock masses and initial stress states on the influence of the support was investigated.

For elastic stress-strain conditions the numerical simulations did match the displacements obtained from the analytical functions. For linear elastic – perfectly plastic stress-strain conditions the numerical simulations deviated from the results obtained with the analytical functions, which underestimate the influence of the support. The proposed correction factor for the influence of the support shows reliable results within the parameter set simulated.

Kurzfassung

Ein wichtiger Faktor für ein erfolgreiches und ökonomisches Tunnelprojekt ist die Vorhersage der Verschiebungsentwicklung im Tunnel um z.B. Nachprofilierungsarbeiten oder zusätzlichen Betonhinterfüllungen aufgrund von Fehleinschätzungen vorbeugen zu können. Die Interaktion zwischen Gebirge und Tunnelausbau spielt dabei eine wichtige Rolle. Die Entwicklung einer verlässlichen Methode zur Verschiebungsprognose hängt wesentlich von der genauen Bestimmung dieser Interaktion ab.
Mittels numerischer 3-D Berechnungen, jeweils für Tunnel mit und ohne Ausbau, wurde die Wirkung des Tunnelausbaus auf die Verschiebungsentwicklung untersucht. Die Ergebnisse dieser Berechnungen wurden mit den Werten analytischer Funktionen verglichen. Durch unterschiedliche Eingabeparameter wurde der Effekt unterschiedlicher Gebirgsarten und Primärspannungszustände auf die Wirkung des Tunnelausbaues untersucht.

Solange das Gebirge nur elastische Verformung erfährt, stimmten die Ergebnisse der numerischen Berechnung mit jenen der analytischen Funktionen überein. Sobald sich jedoch plastische Verformungen einstellen, zeigen die Ergebnisse der numerischen Berechnung eine große Abweichung von den analytischen Berechnungen, die vor allem die Wirkung des Tunnelausbaus sehr unterschätzt. Der vorgeschlagene Korrekturfaktor für die Wirkung des Tunnelausbaus zeigt zufriedenstellende Ergebnisse.

Contents

List of Figures

List of Tables

Abbreviations

σ_r .....radial stress
σ_0.....initial stress
E.....Young's modulus
v .....Poisson's ratio
φ.....friction angle
c .....cohesion
r_p.....plastic radius
a .....tunnel radius
x .....distance between cross section and face
x_s .....point of liner installation
x_f.....value of x at tunnel face
t .....time between cross section and face
t_s .....thickness of the support
L_d .....round length
p_0 .....total pressure acting on the rock mass
p_s .....pressure acting on the support
K.....support parameter
K_s.....ring stiffness of the support
K*.....multiplication factor of K
ΔC_1 .....support displacement
$C_{x\infty}$, X, m, T....Curve fitting parameters

1 Introduction

For a safe and successful tunnel project it is important to have an accurate knowledge of the final displacements and their development with respect to face distance and time. An incorrect displacement prediction can lead to either over-excavation or under-excavation. Both cases can lead to higher cost and delay in completion of the project.
The displacement development due to an underground excavation can be shown with simple formulas, where different factors determine the magnitude and development of the displacement in relation to the excavation advance and time.
For a realistic prediction of the displacements during the construction it is also important to know the influence the tunnel lining, especially shotcrete, has on the displacement development.

1.1 State of the art

There exist several analytical models to describe the general relationship between displacement development, installed support and tunnel advance.

1.1.1 Fenner-Pacher

Fenner (1938) and Pacher (1964) presented one of the first methods to show the ground-support interaction with the so called convergence-confinement method (also called the Fenner-Pacher Curve). Figure 1 shows the convergence line of the rock mass as well as the confinement line of the tunnel support, where the horizontal axis depicts the radial displacement u_r in relation to the tunnel radius r and the vertical axis shows the ratio between the radial stress at the tunnel wall σ_r and the initial stress σ_0. According to Fenner (1938) the convergence line of the rock mass (or ground reaction curve) can be obtained from the elasto-plastic solution for a circular cavity. It also depends on the rock mass parameters. The final equilibrium is given by the intersection of the two lines.
However, this method has certain drawbacks, since it does not include the effect of the tunnel advance. So therefore it is not applicable for predicting the displacement development but can only give the engineer a value for the final displacement.

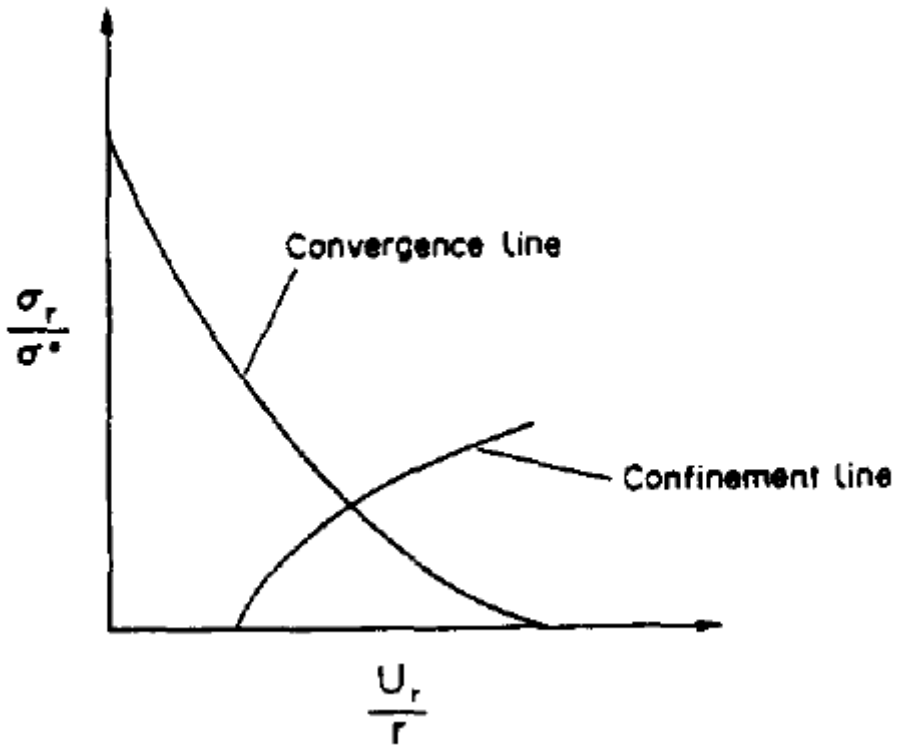

Figure 1: Convergence-confinement lines (taken from Sulem et al. (1987))

1.1.2 Carranza-Torres & Fairhurst

Carranza-Torres & Fairhurst (2000) further developed the convergence-confinement method by introducing the pre-displacements and face-advance dependent displacement development. The upper diagram in Figure 2 shows the face-advance displacement development proposed by Panet & Guenot (1982). In the lower diagram one can see that the ground reaction curve develops linearly between the points O and E and then progresses non-linear until the maximum displacement is reached (point M). Point E represents the critical pressure required for obtaining linear-elastic behaviour. Beyond Point E a plastic zone around the tunnel develops.

As can be seen in Figure 2, the interaction between the rock mass and the tunnel lining is still treated as in the approach by Fenner & Pacher.

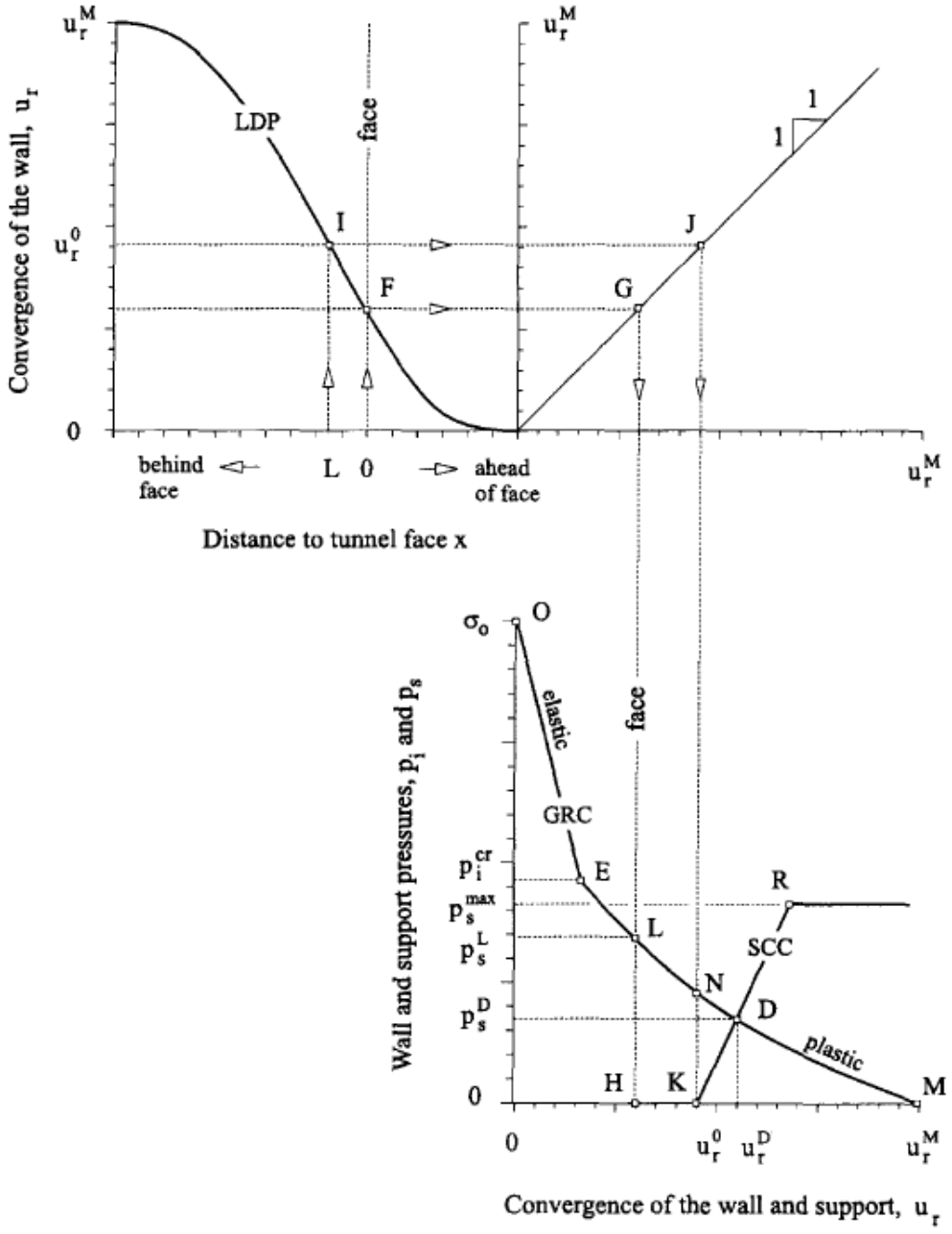

Figure 2: Schematic representation of the Longitudinal Deformation Profile (LDP), Ground Reaction Curve (GRC) and Support Characteristic Curve (SCC) (taken from Carranza-Torres & Fairhurst (2000))

1.1.3 Sulem, Panet & Guenot and Barlow

The method proposed by Sulem, Panet & Guenot (1987) describes the displacement development as a function of time and face-advance. Barlow (1986) extended this method to consider the installed tunnel support (see Chapter 2).

A major drawback of this approach is that the accuracy heavily relies on the correct determination of the different fitting parameters.

1.2 Aim of the work

Nowadays numerical tools are easily accessible but need a lot of time to compute. So therefore a quick and accurate tool to help the site engineer is still of great importance. Sellner (2000) developed such a tool based on the work of Sulem, Panet and Guenot (1987) with the extension for a supported tunnel by Barlow (1986). However the factor K, which represents the support effect on the displacement development, is not known with sufficient accuracy.
In order to be able to describe the influence of the tunnel lining in a more realistic way, it was decided to carry out a number of numerical simulations with varying rock mass parameters.

1.3 Methodology

The following steps were taken in order to fulfill the goals mentioned above:

- Literature study to investigate existing methods for describing the support effect on the displacement development.
- 3-dimensional numerical simulations to determine the displacement development for both unsupported and supported cases.
- Determination of the support factor K for each case and comparison with the analytical result.

2 Basics of Displacement Function

In this chapter the displacement function proposed by Sulem, Panet and Guenot (1987) and the extension by Barlow (1986) is shown. The investigation of the influence of the tunnel lining, which is the aim of this work, will be done using this displacement formulation; therefore a deeper understanding of the equations is needed.

2.1 Basic displacement function

Sulem, Panet and Guenot (1987) proposed a function describing the displacement development of a tunnel in relation to face advance and the time. A number of function parameters is required to establish the displacement curve.
The convergence C is calculated with the following equation:

$$C(x,t) = C_1(x) \cdot [C_{x\infty} + A \cdot C_2(t)] \qquad \text{Eqn. 1}$$

where:

- x distance between observed section and face
- t time elapsed since excavation at observed cross section
- C1(x) time-independent or loading function
- C2(t) time dependent function
- Cx∞ ultimate time-independent convergence
- A ultimate time-dependent convergence

Eqn. 1 shows the basic displacement function, where $C_1(x) * C_{x\infty}$ represents the time-independent displacement. Since $C_1(x) * A * C_2(t)$ represents the time-dependent displacement, one can see that the displacement development is affected by both the elapsed time and the position of the face.

2.1.1 Time dependent displacement

A tunnel deforms time dependent due to the creep deformation of the rock mass. Even when the tunnel advance stops, displacements continue, but usually at a smaller rate. Sulem et al. (1987) described the time dependent part of the displacement function with the following equation:

$$C_2(t) = \left[1 - \left(\frac{T}{T+t}\right)^{0.3}\right] \qquad \text{Eqn. 2}$$

where:

- T curve fitting parameter
- t time between cross section and face

The authors applied this model to actual on-site data from tunnel projects and were able to differentiate the measured convergence between face-advance and time dependent displacements.

2.1.2 Time independent displacement

A tunnel driven in a rock mass causes a change in the static system and equilibrium conditions resulting in time independent displacement.

Panet & Guenot (1982) stated the following about the time independent displacement problem*: "As the face advances, a progressive closure, or convergence, occurs behind the face. The analysis of the convergence on a certain length behind the face is a three-dimensional problem that can be analysed by numerical models. It has been shown that it is possible, considering other uncertainties, to approach this problem by an equivalent plane strain problem"* [see Figure 3].

In the plane strain problem a radial stress, σ_r, is applied on the tunnel wall and is decreased from an initial value equal to the initial stress σ^0 to zero in the case of no support. The temporary support given by the face of the tunnel disappears and tunnel closure increases with distance to the face. The radial stress, σ_r, simulates this face effect and this fictitious temporary support is given by

$$\sigma_r = (1 - \lambda) \cdot \sigma^0$$

where the parameter λ varies from 0 to 1."

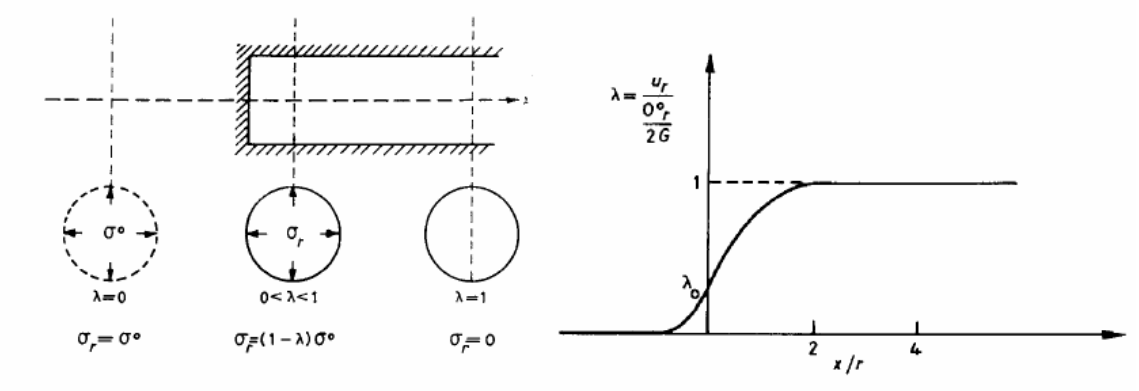

Figure 3: Change of stress during face advance (taken from Panet & Guenot (1982))

After Sulem et al. (1987) the time dependent convergence can be described by Eqn. 3.

$$C_1(x) = \left[1 - \left(\frac{X}{X+x}\right)^2\right] \qquad \text{Eqn. 3}$$

where:

- X curve fitting parameter
- x distance between cross section and face

Finite element analyses by the authors showed that the curve fitting parameter X can be described by the following Equation:

$$X = 0.84 \cdot r_p \qquad \text{Eqn. 4}$$

where:

- X curve fitting parameter
- r_p plastic radius

Note that r_p, used in Eqn. 4 is the plastic radius at an infinite distance from the face where the maximum displacement of the tunnel is reached.

2.1.3 Convergence law

Using Eqn. 2 and Eqn. 3 and the function parameter m which equals $m = A/C_1(x)$, Eqn. 1 can be written as:

$$C(x,t) = C_{x\infty} \cdot \left[1 - \left(\frac{X}{X+x}\right)^2\right] \cdot \left\{1 + m \cdot \left[1 - \left(\frac{T}{T+t}\right)^{0.3}\right]\right\} \qquad \text{Eqn. 5}$$

Eqn. 5 is the so-called convergence law describing the displacement development of a tunnel cross section due to face-advance and time-dependent effects. The shape of the displacement function is governed by the four function parameters: $C_{x\infty}$, X, T and m.

The major drawbacks of this equation are the non-consideration of the influences of the installed tunnel lining and sequential excavation. In the case of a back-calculation with on-site data, the user will only get information of the “complete” tunnel system, meaning the behaviour of the combined rock mass and support system. Any prediction for a specific excavation stage, for example the time between the excavation and the installation of the support, is not possible.

2.2 Extensions by Barlow

In order to overcome the mentioned shortcoming of the convergence law, Barlow (1986) extended the equation to consider sequential excavation and installation of support systems.

2.2.1 Extension for the pre-displacement formulation

Especially for the consideration of sequential excavation but also for taking into account the effect of the installed support more realistically, a profound knowledge of the pre-displacement is needed.
Based on numerical analyses Barlow described the pre-displacement of a given cross section by:

$$C(x,t) = Q_1 \cdot C_{pf}(x) \cdot [C_{x\infty} + A \cdot C_2(t)] \quad \text{Eqn. 6}$$

where:

- Q_1 proportion of the total stress change associated with excavation that occurs ahead of the face
- C_{pf} time independent displacement function ahead of the face

$$C_{pf}(x) = \left[\frac{1}{1 + \left(\frac{x_f - x}{X}\right)}\right]^{1.2} \quad \text{Eqn. 7}$$

where:

- x_f value of x at tunnel face

x_f represents the coordinate at which the observed cross section and the tunnel face are at the same position.
Accordingly the post-face displacement function is altered to:

$$C(x,t) = [Q_1 + Q_2 \cdot C_1(x)] \cdot [C_{x\infty} + A \cdot C_2(t)] \quad \text{Eqn. 8}$$

where:

- Q_2 proportion of the total stress change associated with excavation that occurs behind the face

and:

$$Q_1 + Q_2 = 1 \quad \text{Eqn. 9}$$

The amount of total stress change in the rock mass, shown by C_{pf} in Eqn. 6, increases from zero, when the face is still far ahead of the observed cross section, to Q_1 at x_f. The amount of the total time independent displacement a rock mass has undergone is given by $C_{x\infty} * Q_1$. The time dependent displacement is given by $Q_1 * A * C_2(t)$, but is usually of minor importance, since the time in which the pre-displacements develop is not long enough to reach a noticeable creep behaviour.
A good approach for the value of Q_1 is 0.3, meaning the pre-displacement is about 1/3 of

the total maximum displacement.

2.2.2 Extension for tunnel lining

The introduction of a support system into the excavated tunnel does not change the parameters of the rock mass but it alters the process of stress transfer. This process was investigated by Fenner (1938) & Pacher (1964) (see 1.1.1) and Hoek & Brown (1980).
The tunnel lining shares the load with the rock mass and therefore reduces the load acting on the rock mass, decreasing the displacement. As the tunnel converges, the load on the support increases until a new state of equilibrium is reached. At this point the pressure acting on the lining is $p_{s(final)}$ and the reduced pressure on the surrounding rock mass is equal to $[p_0 - p_{s(final)}]$. The upper diagram of Figure 4 shows the convergence-confinement method with the ground confinement curve (GCC) and the support confinement curve (SCC). In the lower diagram the corresponding convergence curves are shown.

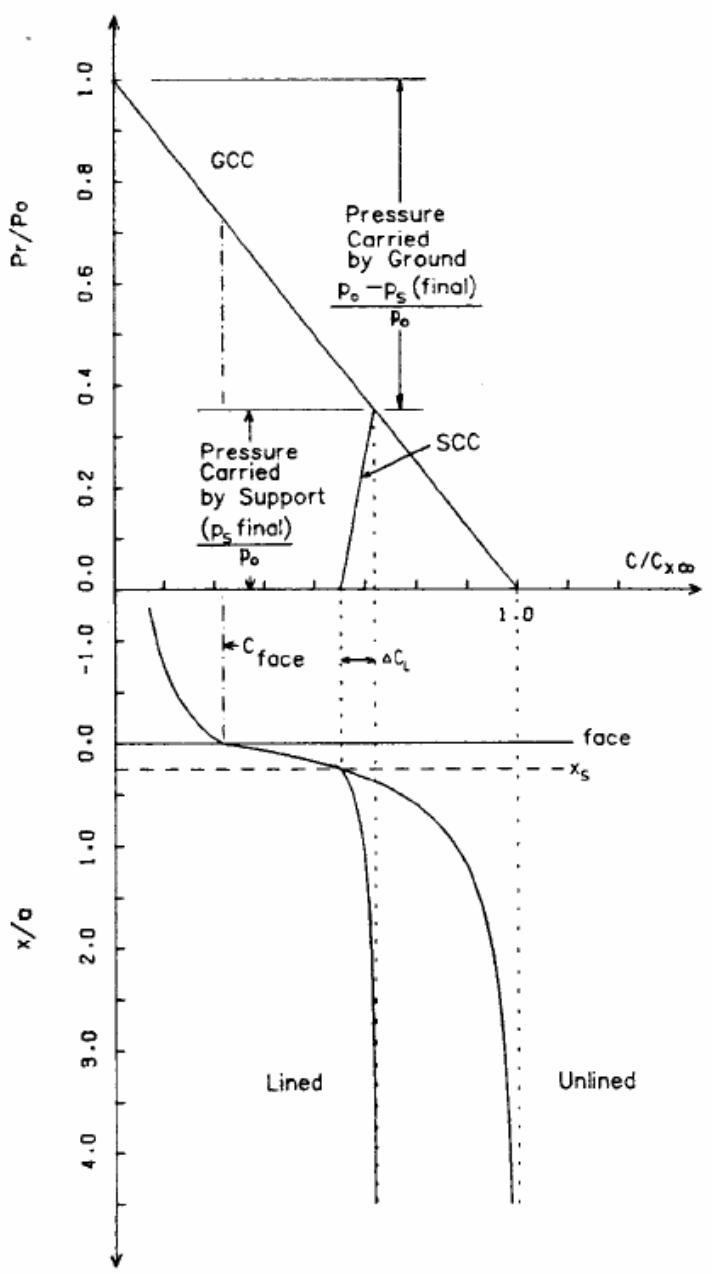

Figure 4: Convergence-confinement method with corresponding convergence curves (taken from Barlow (1986))

Barlow introduced the installation of support into the convergence law by subtracting the resistance developed by the lining, p_s, from the total pressure acting on the rock mass. The modified Eqn. 8 than can be written as:

$$C(x,t) = \left[Q_1 + Q_2 \cdot C_1(x) - \frac{p_s(C(x,t))}{p_0}\right] \cdot [C_{x\infty} + A \cdot C_2(t)] \qquad \text{Eqn. 10}$$

The resistance developed by the support for a given convergence ΔC_1 is given by:

$$p_s\big(C(x,t)\big) = K_s \cdot \frac{\Delta C_1}{2a} \qquad \text{Eqn. 11}$$

where:

- K_s ring stiffness of the support
- a radius of the tunnel

According to Hoek & Brown (1980) the ring stiffness of the support is given by:

$$K_s = \frac{E_s \cdot (a^2 - (a - t_s)^2)}{(1 + v_s) \cdot [(1 - 2v) \cdot a^2 + (a - t)^2]} \qquad \text{Eqn. 12}$$

where:

- E_s Young's modulus of the support
- t_s thickness of the support
- v_s Poisson's ratio of the support

Substituting Eqn. 11 in Eqn. 10 and simplifying gives:

$$C(x,t) = \frac{[Q_1 + Q_2 \cdot C_1(x) + K \cdot C_s]}{[1 + K \cdot (C_{x\infty} + A \cdot C_2(t))]} \cdot [C_{x\infty} + A \cdot C_2(t)] \qquad \text{Eqn. 13}$$

where:

- C_s convergence at the point of support installation

and

$$K = \frac{K_s}{2 \cdot a \cdot p_0} \qquad \text{Eqn. 14}$$

where:

- K support parameter
- p_0 initial stress acting on the rock mass

These equations now split the displacement function in 3 parts:

The pre-displacements (Eqn. 6), the part between the face and the installation of the support (Eqn. 8), and the section after the support installation (Eqn. 13). In these

equations only the factor K in Eqn. 13 describes the influence of the tunnel lining and the displacements before the installation of the support are not influenced by it at all. Since this is not realistic, another modification of the convergence law is required. To consider the effect of the support system ahead of its installation Barlow introduced the functions P_k^- and P_k^+ and the factor Q_k.

P_k^- and P_k^+ are defined as:

$$Q_k \cdot P_k^+(x) = Q_k \cdot \left[\frac{X}{X + (x_s - x)}\right]^{\alpha} \qquad \text{Eqn. 15}$$

$$Q_k \cdot P_k^-(x) = Q_k \cdot \left[\frac{X}{X + (x - x_s)}\right]^{\alpha} \qquad \text{Eqn. 16}$$

where:

x_s point of liner installation

and

$$\alpha = 1 + \frac{a}{L_d}$$

where:

L_d round length

P_k^- is equal to 1 at the point of liner installation x_s and decreases to zero far behind the face. In the same manner P_k^+ decreases from 1 at x_s to zero at a point far ahead of the face. Therefore, the installation of the tunnel support has an effect on the displacement development ahead and behind its point of installation.

The factor Q_k is equivalent to the maximum displacement reduction due to the installation of the support at the tunnel face ($x = x_f$). Its value can be in the range of 0 to 1. According to Barlow the value of Q_k decreases with decrease in liner stiffness and with an increase in support installation delay.

Introducing Eqn. 15 and Eqn. 16 into Eqn. 6,Eqn. 8 and Eqn. 13 gives the extended convergence law by Barlow with 3 displacement sequences:

- Pre-displacement ($x<x_f$):

$$C(x,t) = [Q_1 \cdot C_{pf}(x) - Q_k \cdot P_k^+(x)] \cdot [C_{x\infty} + A \cdot C_2(t)] \quad \text{Eqn. 17}$$

- Post-face pre-liner displacement ($x_f<x<x_s$):

$$C(x,t) = [Q_1 + Q_2 \cdot C_1(x) - Q_k \cdot P_k^+(x)] \cdot [C_{x\infty} + A \cdot C_2(t)] \quad \text{Eqn. 18}$$

- Post-liner displacement ($x \geq x_s$):

$$C(x,t) = \frac{[Q_1 + Q_2 \cdot C_1(x) + K \cdot C_s - Q_k \cdot P_k^-(x)]}{[1 + K \cdot (C_{x\infty} + A \cdot C_2(t))]} \cdot [C_{x\infty} + A \cdot C_2(t)] \quad \text{Eqn. 19}$$

Figure 5 shows a displacement plot using Barlow's equations for both an unlined and a lined case. The two curves are identical up to the point of liner installation at a distance to face of around 2 meters. The support then decreases the displacement development, as can be seen in Figure 5.

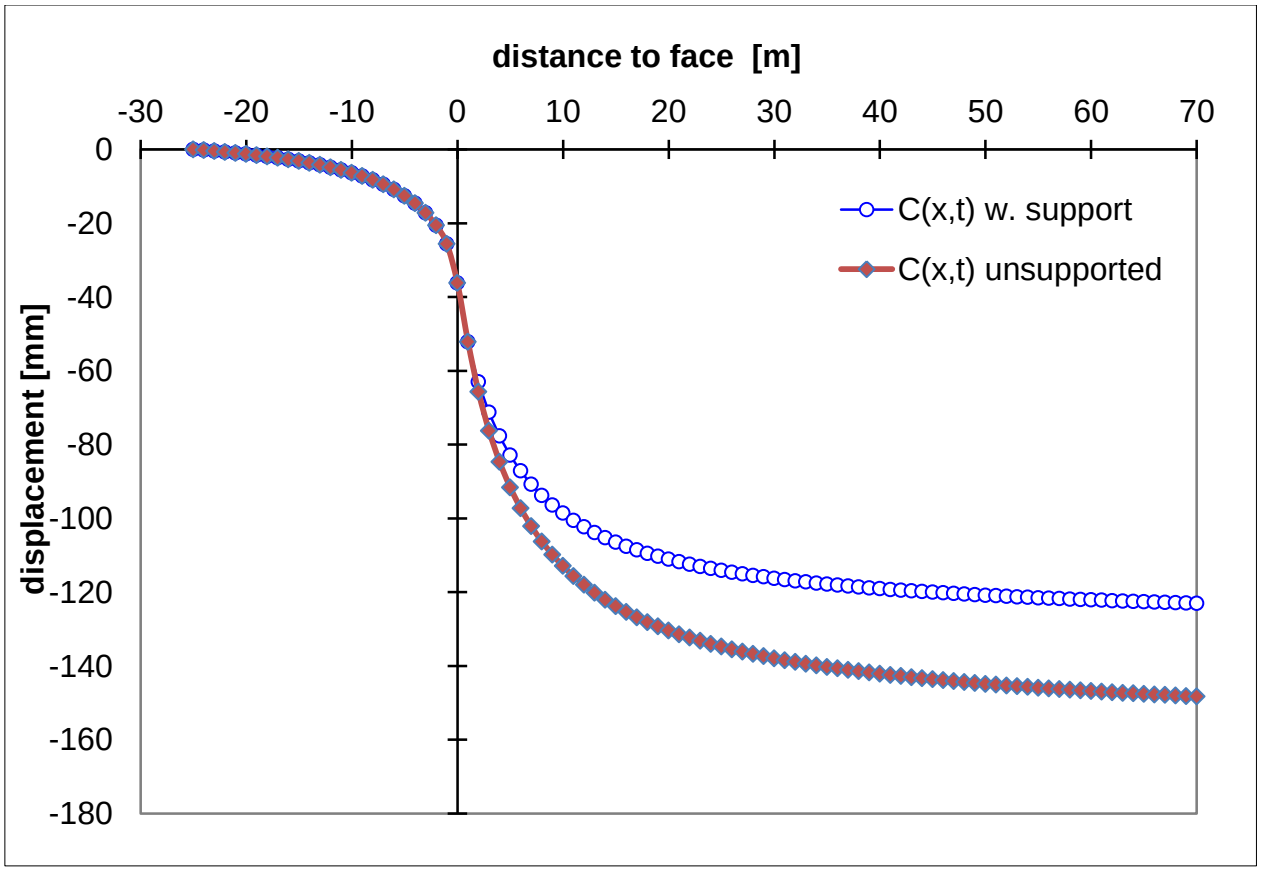

Figure 5: Displacement development for an unsupported and supported tunnel

2.2.3 Modification by Sellner (2000)

Sellner (2000) in his doctoral thesis proposed a modification of the support parameter K to overcome shortcomings of Barlow's formulation. Based on a series of numerical simulations with varying rock masses and support parameters he developed a correction factor y for the calculation of K (see Eqn. 20 and Eqn. 21).

$$K_{mod} = \frac{K}{y} \qquad \text{Eqn. 20}$$

$$y = A \cdot \left(\frac{\sigma_{sidewall}}{UCSm}\right)^{E} \qquad \text{Eqn. 21}$$

where:

K_{mod}	modified value of K
A, E	constants for support
$\sigma_{sidewall}$	stress acting on the tunnel wall
UCSm	unconfined compressive strength of the rock mass

Sellner's modification factor increases the support parameter K for any rock mass with a small factor of utilisation and decreases K with increasing factor of utilisation, as it can be seen in Figure 6.

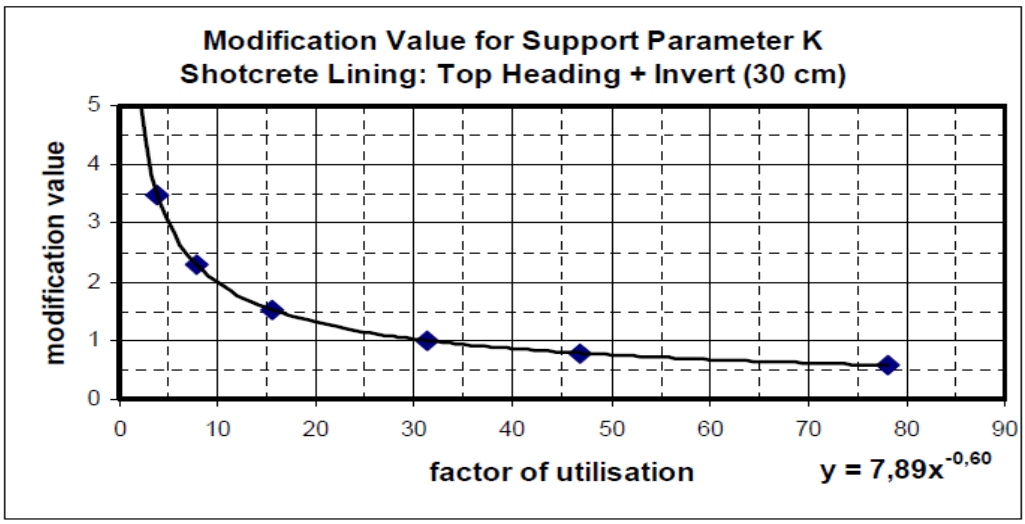

Figure 6: Value of the modification factor y for the support parameter K (taken from Sellner (2000))

3 Numerical model setup

The program used for the numerical calculations in this thesis was FLAC^{3D} from Itasca Consulting Group Inc. FLAC^{3D} is a three-dimensional explicit finite-difference program specially designed for investigating geotechnical problems.

The dimensions of the model for the full-face excavation calculations are 30m in height and width (x- and z-axis) and 70m in length (y-axis) (see Figure 7). The radius of the tunnel is 5 meters. The spacing of the mesh in y-direction was set to 1 meter so that it corresponded to the chosen round length of also 1m.

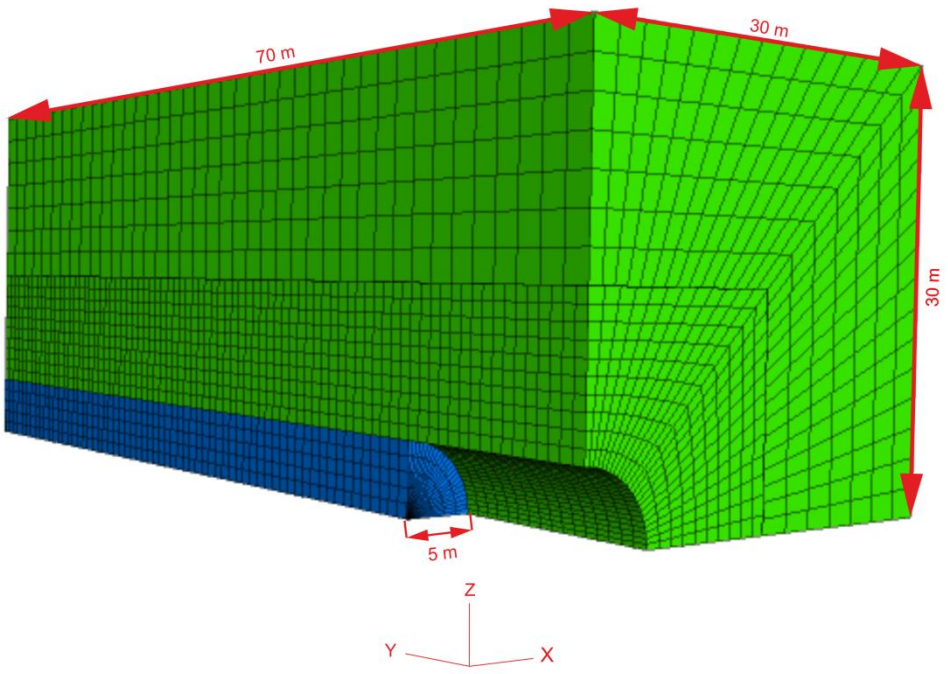

Figure 7: Numerical Model setup

The tunnel was divided into cross sections every meter (corresponding to the longitudinal mesh spacing and the round length). Every cross section had 3 measuring points along its perimeter (see Figure 8) and during the tunnel advance the displacements in x-,y- and z-direction were calculated for every measuring point in each cross section.

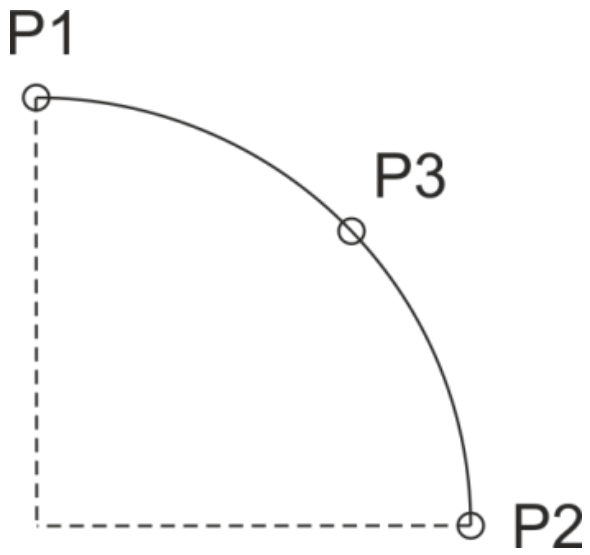

Figure 8: Cross section with measuring points

Some test calculations were necessary to determine the required length for the model so that a cross section in the middle of the model will reach its final displacement. Final displacement was reached when there was no increase in the displacement with advancing tunnel face.
For calculations with supported tunnels the setup was equal except for the tunnel length. Since the final displacement of a supported tunnel is less than of an unsupported, a model length of 50 meters fulfilled the above stated displacement criterion. The shortening of the model was done to reduce calculation time.

The support was installed one round length behind the face. The support was modelled as an elastic material with no failure limit.

For the rock mass Mohr-Coulomb constitutive model was used in the calculations assuming linear elasticity and perfect plasticity; hydrostatic stress conditions were assumed.
In order to reduce calculation time significantly, the axial symmetry of the entire problem was used. A symmetry boundary along the x- and z-axis was defined.

Since FLAC^{3D} is a finite difference program, it uses approximations to solutions to differential equations. The computation of these approximations is an iterative process, therefore it is essential to define an equilibrium criterion. Itasca's recommended criterion is a ratio between maximum unbalanced force and total applied forces smaller than 10^{-5}. To get a more accurate result while maintaining a reasonable calculation time the equilibrium criterion was altered to a maximum ratio of 10^{-6}.

3.1 Sequential Excavation

For the calculations with sequential excavation a different model setup was used. Due to the more complex geometry, the mesh was generated with the program ABAQUS/CAE (Dassault Systèmes Simulia Corp.) and then imported into FLAC^{3D}. The use of a model with only a quarter of the tunnel was not possible, therefore it was changed to a model with the dimensions of 30m in x- direction and a height of 60m and a symmetry plane along the y-z-plane (see Figure 9). The length was set to 80 meters to fulfill the displacement criterion described in section 3. The tunnel radius was again 5 meters.

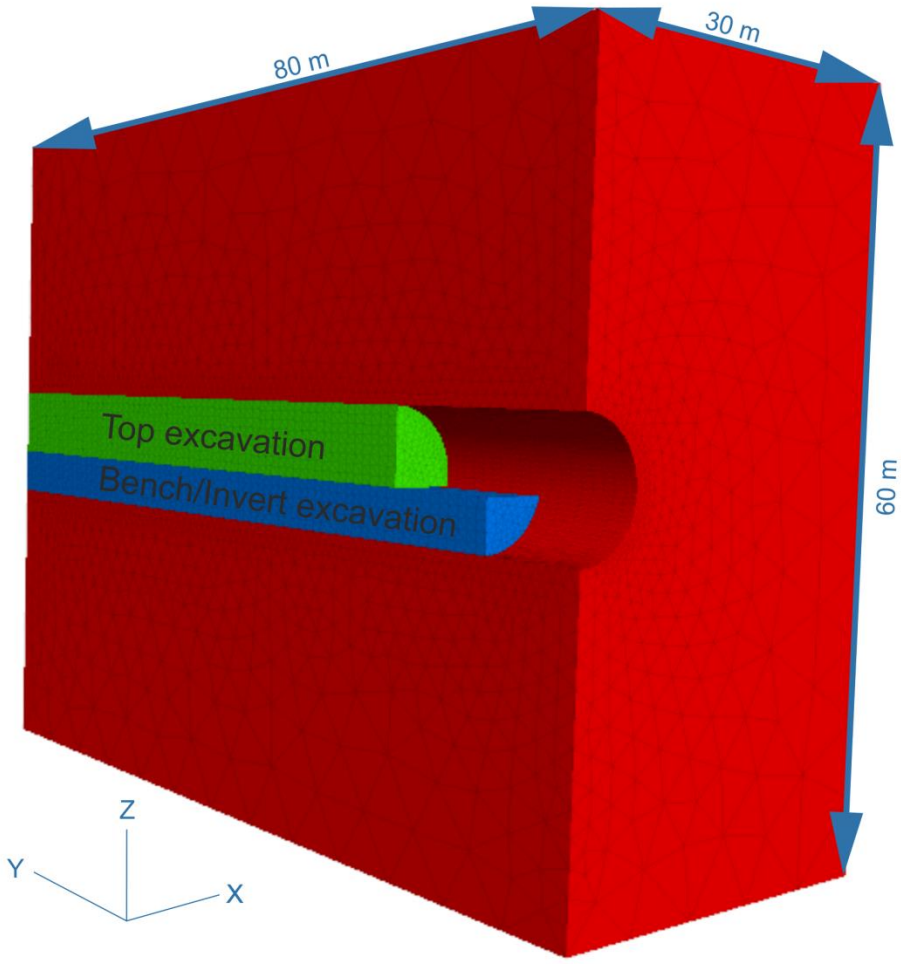

Figure 9: Numerical model setup - sequential excavation

Like in the full-face excavation, the face advanced with 1 meter per excavation step. The cross section was divided into two parts, the top and the bench/invert. The top had a height of 6 meters at the tunnel axis and the bench/invert height was 4 meters (see Figure 10). The distance between the top and the bench/invert excavation faces varied and was

set to 5, 10 and 20 meters. The installation of the support was done one round length behind the face advance for each segment. The support parameters were the same as for the full-face excavation.

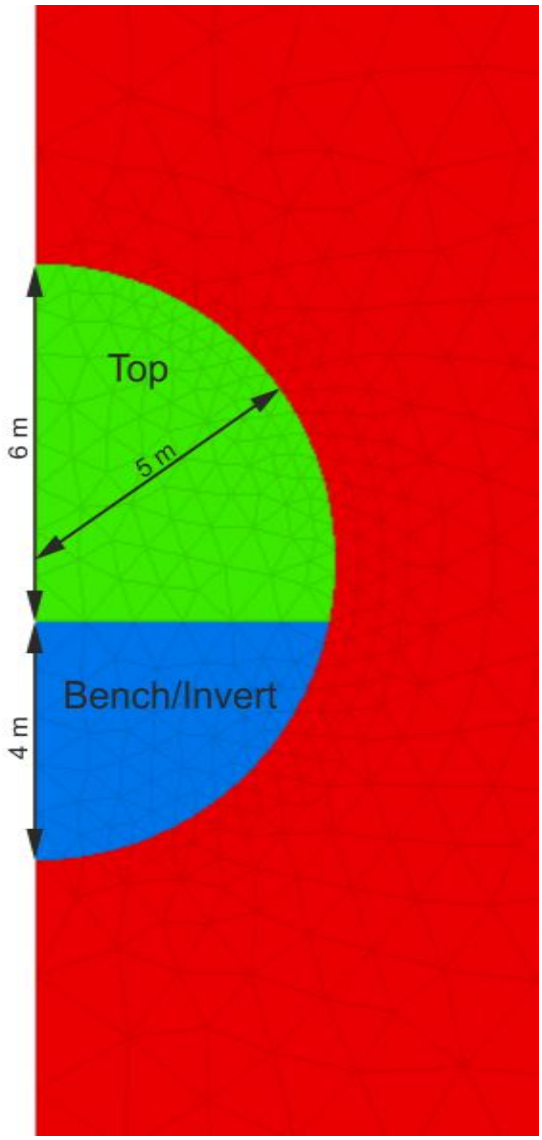

Figure 10: Cross-section - sequential excavation

4 Numerical Analysis

To investigate the influence of supports on the displacement development one needs to examine a supported and an unsupported tunnel with exactly equal geological and geotechnical parameters. This can only be provided with a numerical analysis.

The analysis focused only on the time-independent part of the displacement development, since the tunnel lining doesn't have much influence on the time-independent displacements. No creep function has been implemented in the numerical model and in the convergence law, the displacements due to creep were neglected by setting the time-dependent function parameters (m and T, see Chapter 2.1.2) to m = 0.

4.1 Calibration

Before performing the numerical analysis a testing of the setup was performed to see if it corresponds to the analytical solution by Sulem et al. (1987) and Barlow (1986) (see Chapter 2).

4.1.1 Modification of the support parameter K

When Barlow developed his formulation of the support parameter K (see Chapter 2.2.2) tunnel displacement was measured as relative displacement (convergence measurements). Now geodetic measurements have replaced the convergence measurements and give the user the displacements separately for each point. The numerical setup used in this thesis also shows absolute displacements.
Therefore Barlow's function of the effect of the tunnel lining has to be modified.
Eqn. 11 was slightly modified to take the different measurement method into account:

$$p_s\big(C(x,t)\big) = K_s \cdot \frac{\Delta C_1}{a} \qquad \text{Eqn. 22}$$

where:

- p_s resistance developed by the lining
- K_s ring stiffness of the support
- ΔC_1 support displacement
- a radius of the tunnel

This modification changed the function for the support parameter K (Eqn. 14) to the following form:

$$K = \frac{K_s}{a \cdot p_0} \qquad \text{Eqn. 23}$$

where:

- p_0 initial stress acting on the rock mass

Eqn. 23 is the new formulation of Barlow's support parameter K for absolute displacement measurements.

4.1.2 Results

The calibration was done with a rock mass that only exhibits elastic behaviour during the procedure. Table 1 shows the material properties of the rock mass. The in-situ stress σ^0 was set to 18.75 MPa which represents an overburden of around 750 meters.

Table 1: Elastic material properties

E [MPa]	K [MPa]	G [MPa]	v [-]	phi [°]	c [MPa]
1000	666,666	400	0,25	35	5

With the closed form solution by Feder & Arwanitakis (1976), the combination of rock mass and overburden was checked if plastic zones occur.

The support was modelled as a shotcrete lining with a Young's modulus of 4000 MPa, a Poisson's ratio of 0.25 [-] and a thickness of 20 cm (see Table 2).

Table 2: Support parameters

E [Mpa]	v [-]	t[m]
4000	0,25	0,2

Figure 11 and Figure 12 show the comparison between the numerical results and the analytical function by Sulem et al. (1987) and Barlow (1986).

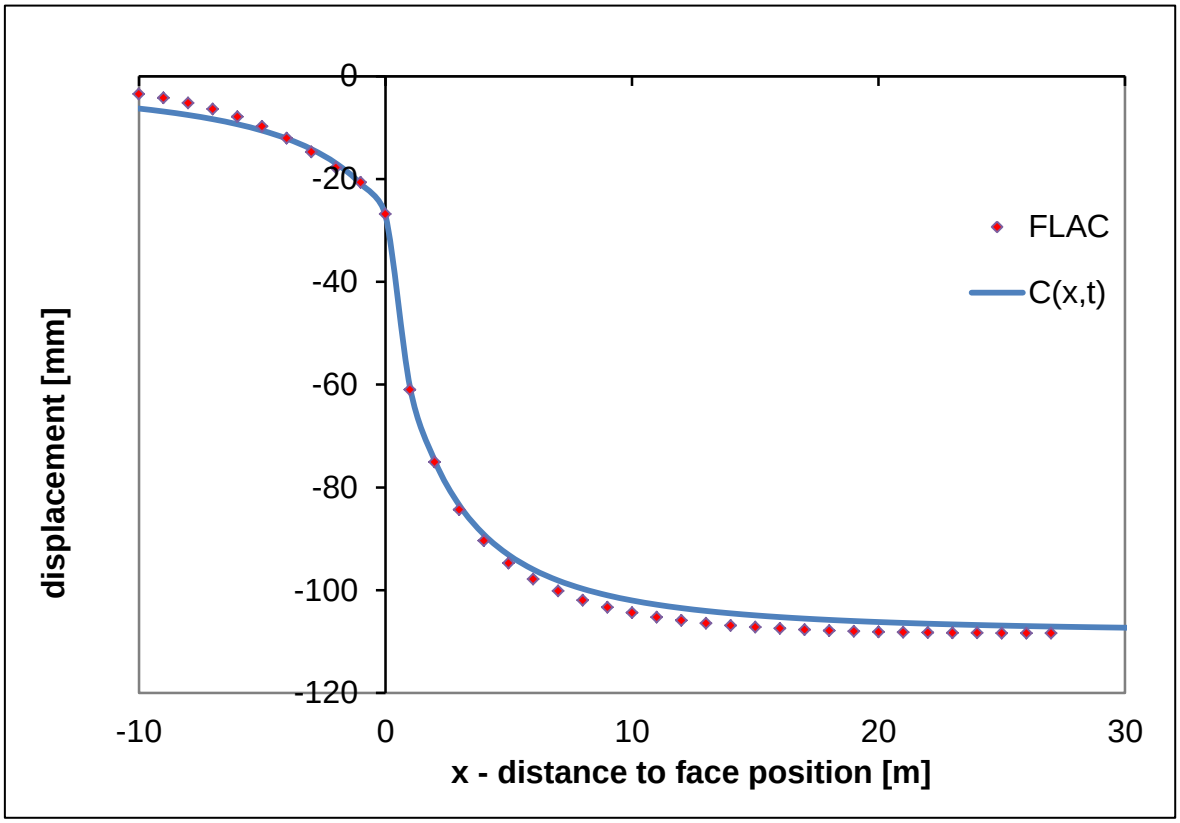

Figure 11: Comparison between convergence law and numerical results - unsupported

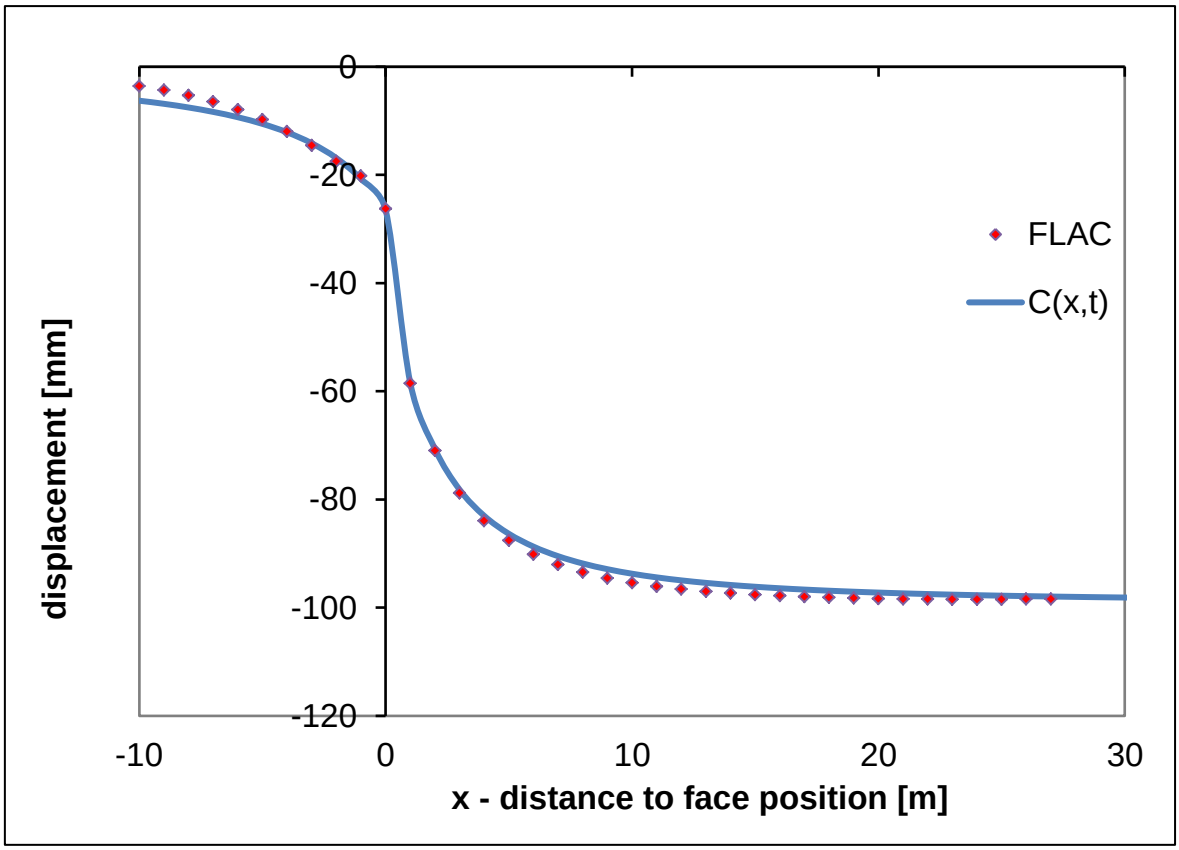

Figure 12: Comparison between convergence law and numerical results – supported

As it can be seen both the unsupported as well as the supported tunnel displacements almost perfectly fit to the convergence law, especially in the displacements behind the face.

However, the convergence law reaches its final displacement at an infinite distance to the face which is not realistic, since no tunnel is infinitely long. To overcome this problem and obtain an even better fit with the FLAC^{3D} results, the convergence law displacement function (C(x,t)) was normalised by the displacement at 98% of the maximum displacement. This was accomplished by applying following equation:

$$\overline{C}(x,t) = \frac{C(x,t)}{C_{98}(x,t)} \cdot C_{max}(x,t) \qquad \text{Eqn. 24}$$

where

$\overline{C}(x,t)$ modified displacement function

$C_{98}(x,t)$ displacement at 98% of the maximum displacement

$C_{max}(x,t)$ maximum displacement at infinite distance to the face

Figure 13 and Figure 14 show the now improved fitting between the modified convergence law and the numerical results.

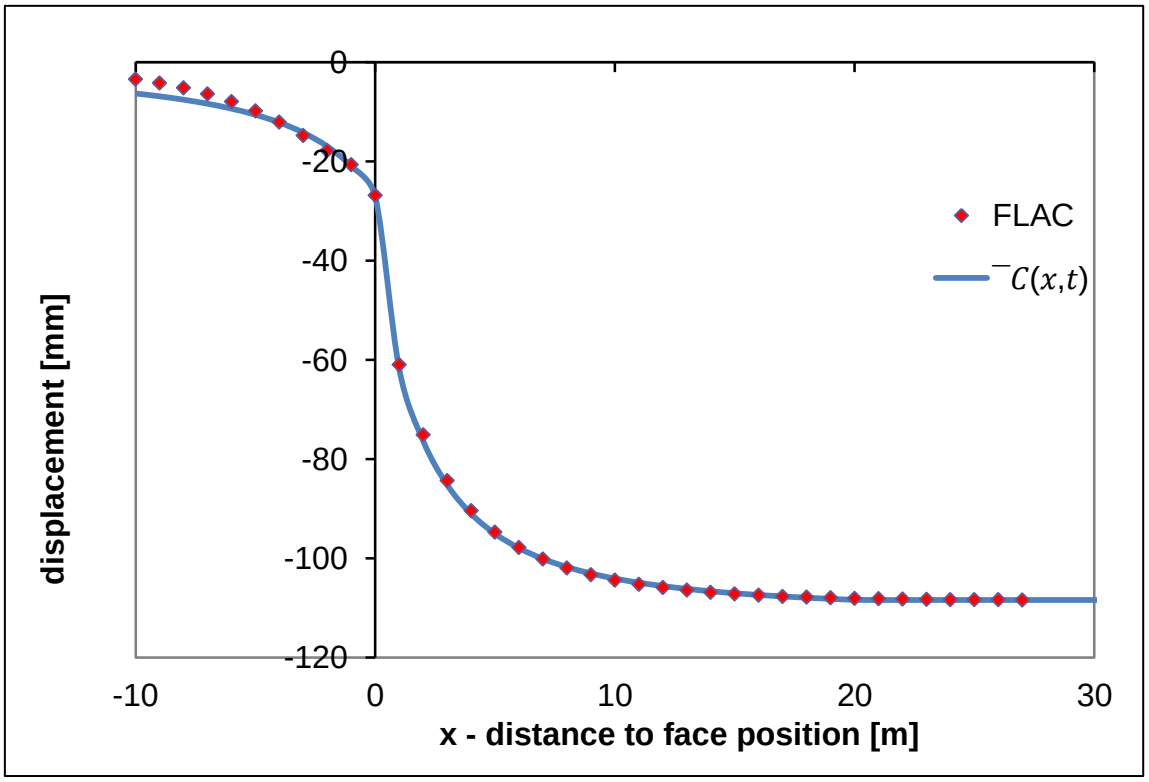

Figure 13: Comparison between modified convergence law and numerical results – unsupported

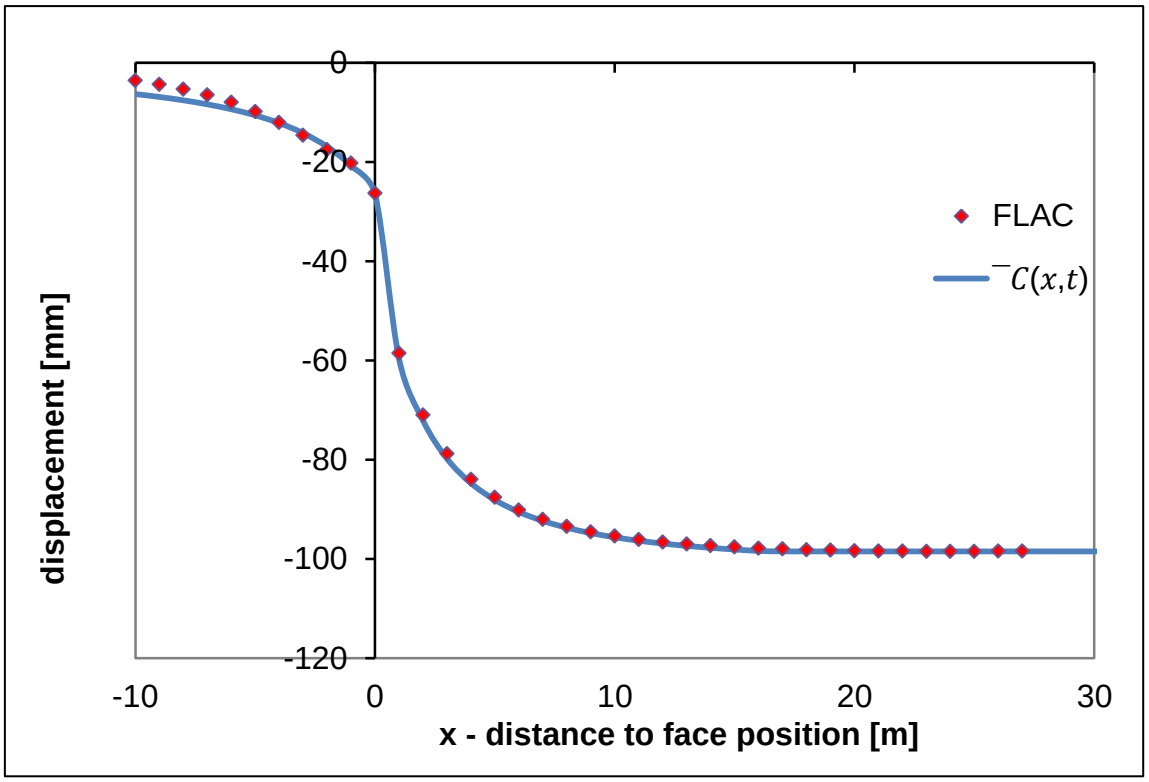

Figure 14: Comparison between modified convergence law and numerical results – supported

4.2 Calculations

Barlow's only used linear elastic material behaviour in his calculations. Results shown in Chapter 4.1.2 match well with his formulation and linear elastic numerical simulations. However rock mass rarely behaves only in a linear elastic way, therefore the calculations of this thesis were performed using Mohr-Coulomb material law (linear elastic – perfectly plastic).

Three rock mass types (RM 1 to 3) were chosen to investigate the effect of the support. The material parameters are listed in Table 3.

Table 3: Rock mass parameters

RM	E [Mpa]	K [Mpa]	G [Mpa]	v [-]	φ [°]	c [Mpa]
RM1	2000	1333,33	800	0,25	27	0,5
RM2	300	200	120	0,25	35	0,03
RM3	150	100	60	0,25	25	0,07

Unfortunately RM2 and RM3 were too “weak” for the numerical setup, meaning FLAC^{3D} couldn’t find a state of equilibrium, which fulfilled the chosen equilibrium criterion. The effect of the support could be investigated with RM1 and three different initial stress states were used (ST 1 to 3). Table 4 gives the values of the different stress states and their corresponding overburden.

Table 4: Stress states and corresponding overburden

stress state	σ_0 [Mpa]	overburden (aprox.) [m]
ST1	2,7	100
ST2	6,75	250
ST3	13,5	500

As it can be seen in Figure 15 and Figure 16 the fitting between the numerical results and the convergence law are not as good as they were with the linear elastic material. Especially the support’s effect on the displacement development diverges significantly between the numerical simulation and Barlow’s formulation (Figure 16).

The plausibility of the obtained results from FLAC3D was checked with the two-dimensional finite element program Phase2 (rocscience inc.). The maximum displacement for the same material parameters was about the same in both programs, therefore the results from the FLAC3D-analysis were considered plausible.

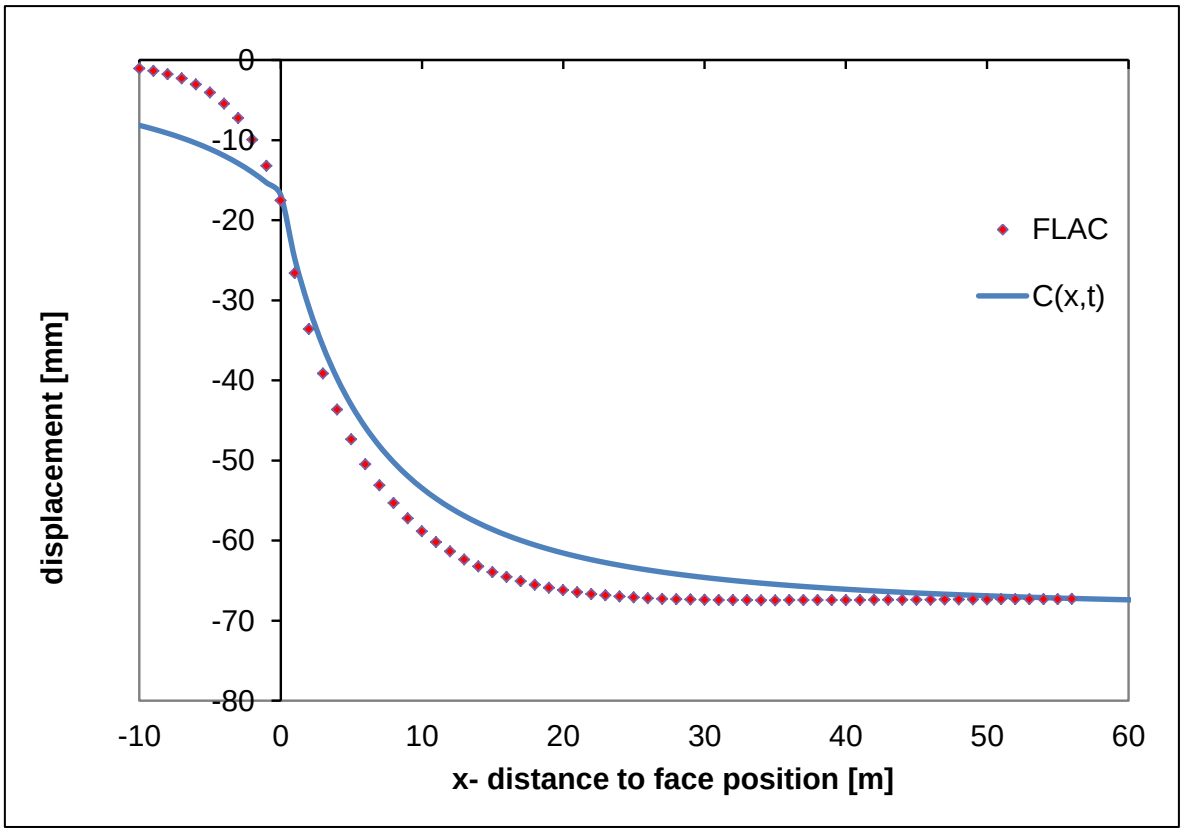

Figure 15: Comparison RM1 with convergence law (stress state 2) – unsupported

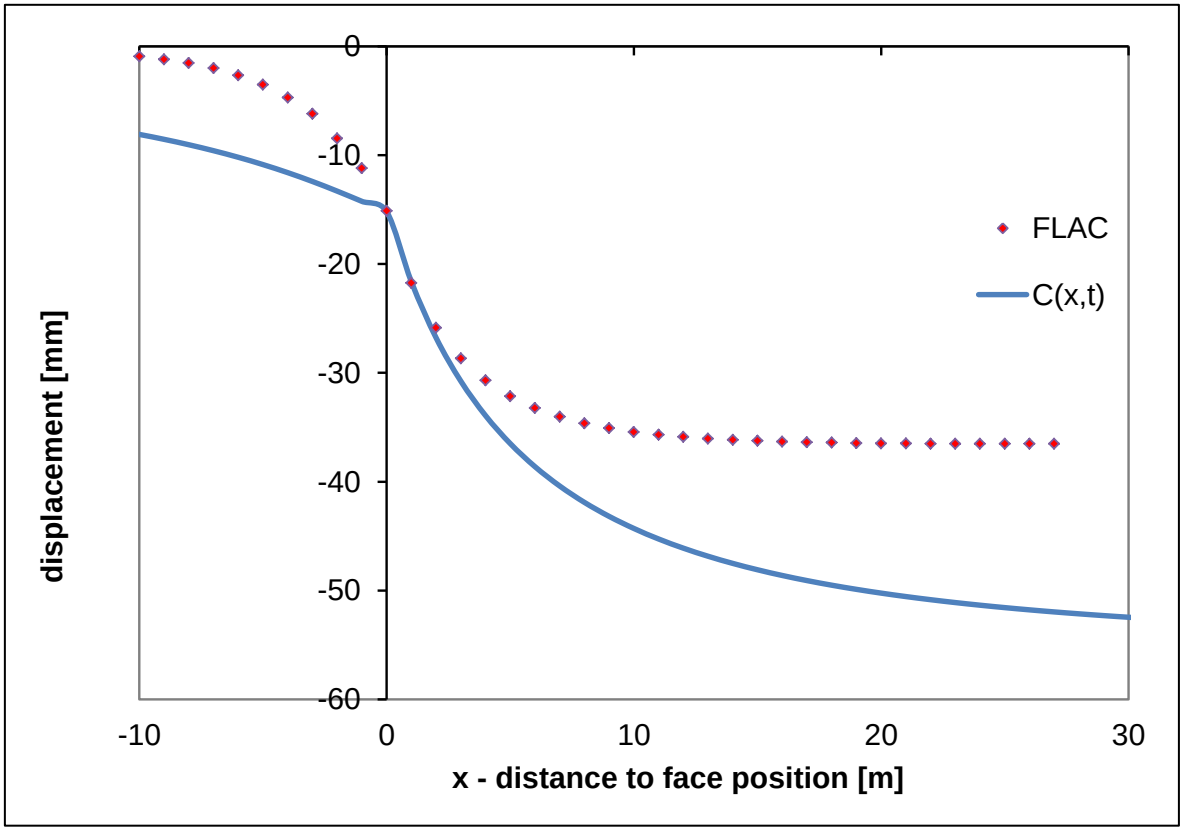

Figure 16: Comparison RM1 with convergence law (stress state 2) – supported

Figure 15 and Figure 16 show that the formulations by Sulem et al. (1987) and Barlow (1986) don't hold true for plastic behaviour of the rock mass. The aim of this thesis though, was not to establish a new convergence law, but to adjust the parameters of the existing formulation to arrive at a good fitting to rock masses with plastic behaviour.

The following parameters were changed in order to obtain a better fitting between the FLAC^{3D} results and the convergence law: X, Q_k, C_{pf} and K.

- X is the time-independent fitting parameter (see Eqn. 3 and Eqn. 4). The proposed value of X in Eqn. 4 works as a good approximation.

- Q_k describes the influence of the support on the displacements ahead of the point of its installation (see Eqn. 15 and Eqn. 16). Sellner (2000) proposed a value of Q_k of 0.04.

- C_{pf} is the time-independent displacement function ahead of the face (see Eqn. 7). In this work the exponent of Eqn. 7 (value of 1.2) was modified to fit the pre-displacements

- The effect of the support is represented by K (see chapter 2.2.2). The value of K, proposed by Barlow (1986) and modified in chapter 4.1.1, holds true for elastic behaviour, but is far from accurate for plastic deformation. For a better fitting of the supported displacement curves, K (Eqn. 23) was multiplied by the factor K*

In Table 5 the changed fitting parameters are listed for each stress state. Also the corresponding plastic radius r_p and the fitting parameter C, which governs the final displacement, are shown in Table 5

Table 5: Fitting parameters RM1

RM	stress state	C	X	Q_k	K*	exp. of C_{pf}	r_p
RM1	1	-11,3	5,5	0,02	3	2	7,7
	2	-67,46	8	0,06	6	3	12,02
	3	-252,4	12	0,09	7	4	17,54

As can be seen in Figure 17 for the unsupported and Figure 18 for the supported case, the fitting between the function C(x,t) and the numerical results is now almost perfect. The effect of the support for stress state 2 is 6 times higher than the proposed value of K according to Eqn. 23.

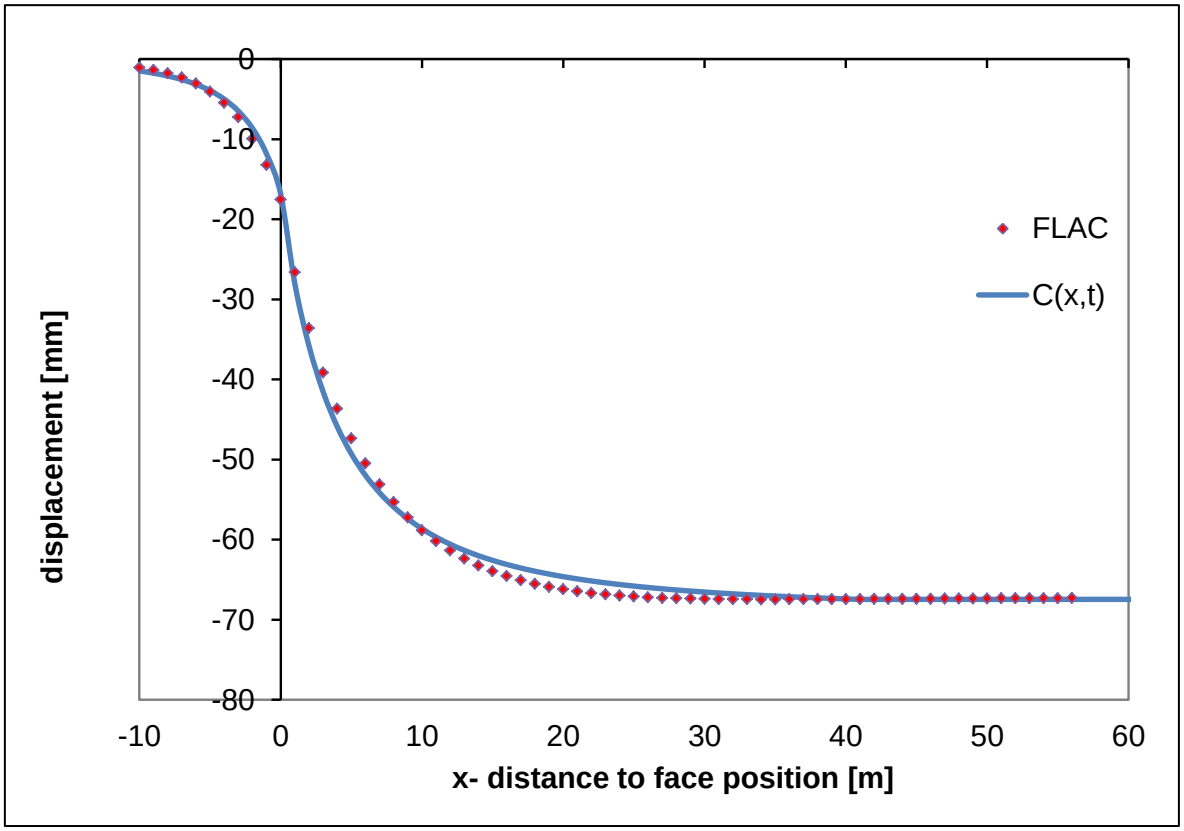

Figure 17: Comparison RM1 with fitted convergence law (stress state 2) – unsupported

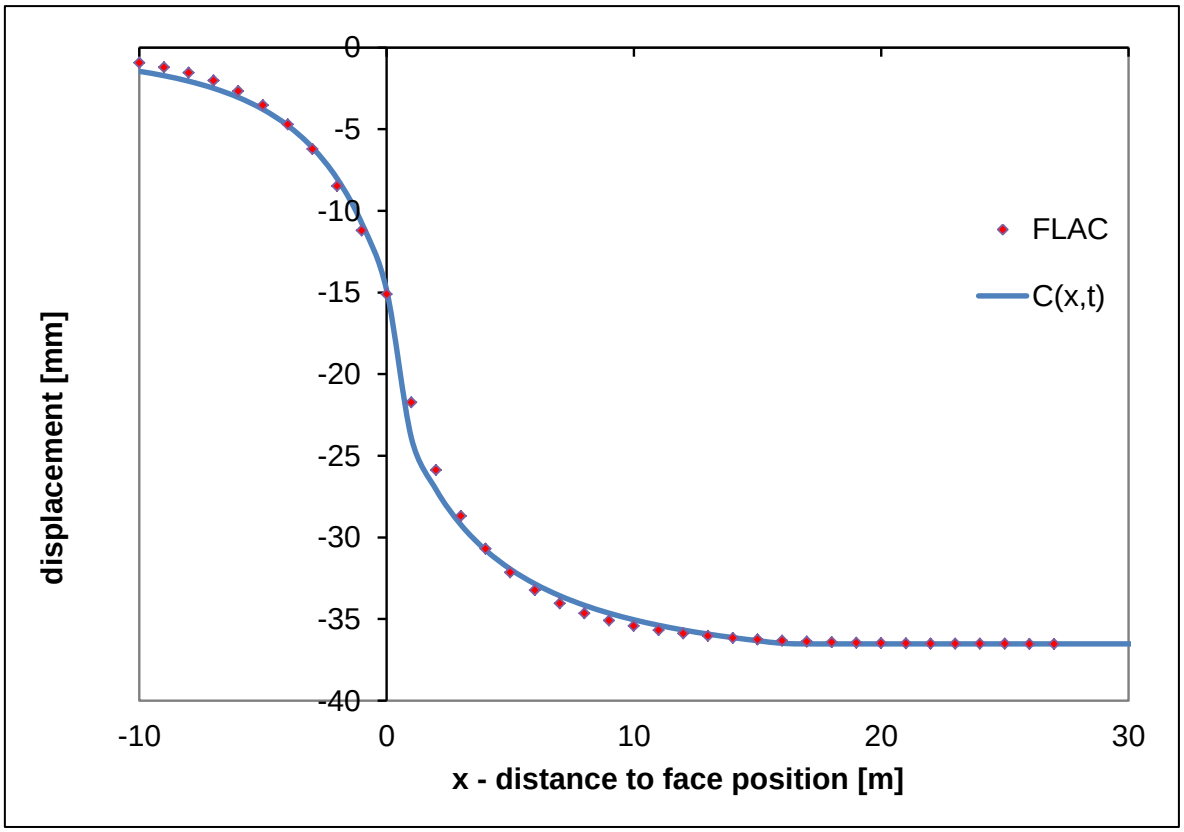

Figure 18: Comparison RM1 with fitted convergence law (stress state 2) – supported

Based on the findings from RM1 a parameter study of the rock mass parameters was carried out. Friction angle phi (RM1_phi), Young's modulus E (RM1_E) and cohesion c (RM1_c) were changed according to the values in Table 6. Note that FLAC3D requires to enter the elastic moduli in terms of bulk modulus K and shear modulus G. Therefore a change of Poisson's ratio ν was not performed because the change of E already resulted in different values of K and G.

Table 6: Rock mass parameters

RM	E [Mpa]	K [Mpa]	G [Mpa]	v [-]	φ [°]	c [Mpa]
RM1	2000	1333,33	800	0,25	27	0,5
RM1_phi	2000	1333,33	800	0,25	35	0,5
RM1_E	6000	4000	2400	0,25	27	0,5
RM1_c	2000	1333,33	800	0,25	27	2

For each “new” rock mass (RM1_phi, RM1_E and RM1_c) the same stress states (see Table 4) as for RM1 were applied. The results of this study are listed in Table 7.

Table 7: Fitting parameters – parameter study

RM	stress state	C	X	Q_k	K*	exp. Of C_{pf}	r_p	K
RM1	1	-11.3	5.5	0.02	3	2	7.7	-0.039
	2	-67.46	8	0.06	6	3	12.02	-0.031
	3	-252.4	12	0.09	7	4	17.54	-0.018
RM1_phi	1	-9.11	5	0.02	2.5	2	6.52	-0.033
	2	-40.3	6.5	0.04	5.5	2.5	8.71	-0.029
	3	-134.4	9	0.1	7.5	3	11.07	-0.020
RM1_E	1	-3.78	5.5	0.02	3	2	7.7	-0.039
	2	-22.5	8.5	0.04	6	3	12.02	-0.031
	3	-84.12	12	0.08	7	4	17.54	-0.018
RM1_c	1	-7.46	4.2	0.02	1	1.5	5	-0.013
	2	-22.25	5	0.02	2	2	6.34	-0.010
	3	-70.56	6	0.03	3	3	8.52	-0.008

RM1_c in stress state 1 did not develop any plastic deformation (as indicated by a plastic radius equalling the tunnel radius) so only the parameters dictating the pre-displacements (Q_k and C_{pf}) were slightly changed. Note that a changed Young’s modulus, as represented by the rock mass RM1_E did not change the support parameter K. Therefore the results of RM1_E are not displayed in the following graphs.

Figure 19 shows the support parameter K in relationship with the plastic radius for the different rock masses. The three solid lines represent the value of K proposed by Barlow for the three stress states. Barlow’s value of K is constant for every plastic radius or set of rock mass parameters. The difference between the Barlow’s value and the K values obtained from the numerical simulations varies for every stress state but as Figure 20 shows, the multiplication factor of K, K*, increases with increasing plastic radius. But the highest K*-value was obtained with RM1_phi, although this rock mass doesn’t have the largest plastic radius.

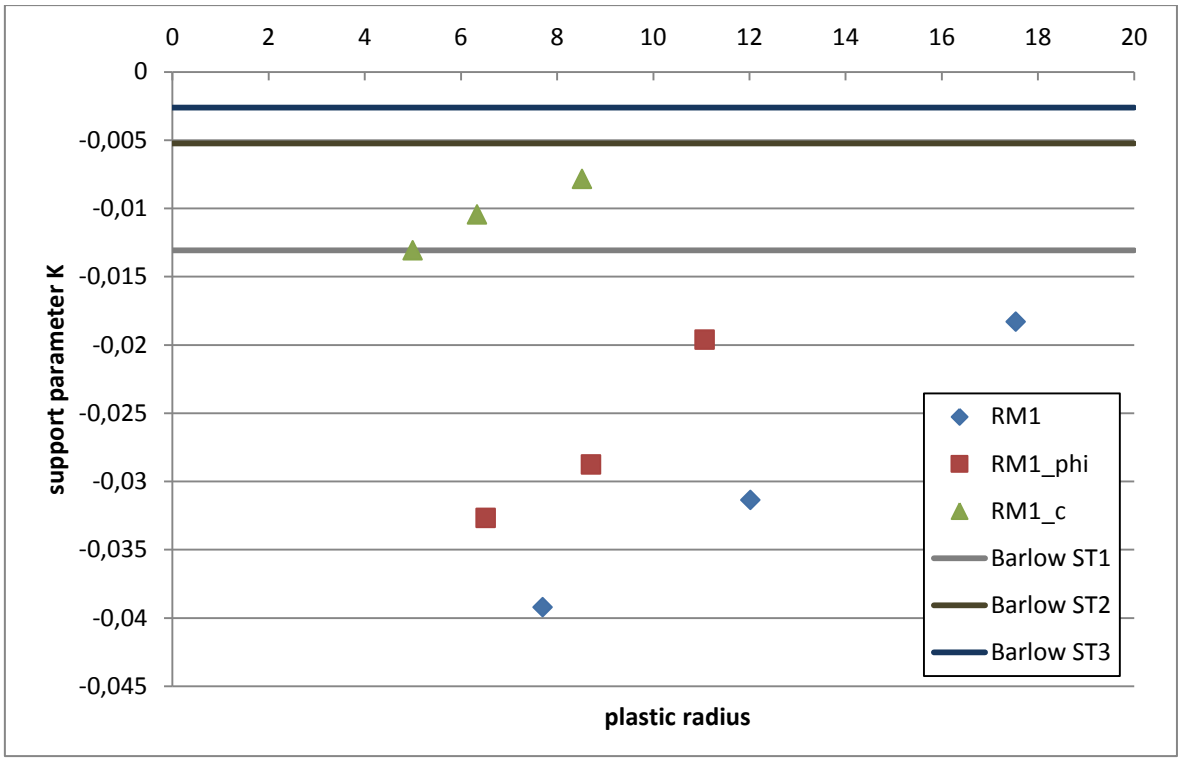

Figure 19: Relationship between plastic radius and support parameter K

The curve fitting parameter X increases almost linearly with increasing plastic radius (see Figure 21).

The support's influence ahead of its point of installation Q_k showed a similar behaviour, although until a plastic radius of 7.7m the value was constant and beyond this point it increased. But again, the maximum plastic radius didn't cause the highest value of Q_k but rock mass RM1_phi did (see Figure 22).

The relationship between the plastic radius and the exponent of the time-independent pre-displacement function C_{pf} is almost linear, with the exponent of C_{pf} starting at a value of 1.5 and a maximum value of 4 (see Figure 23).

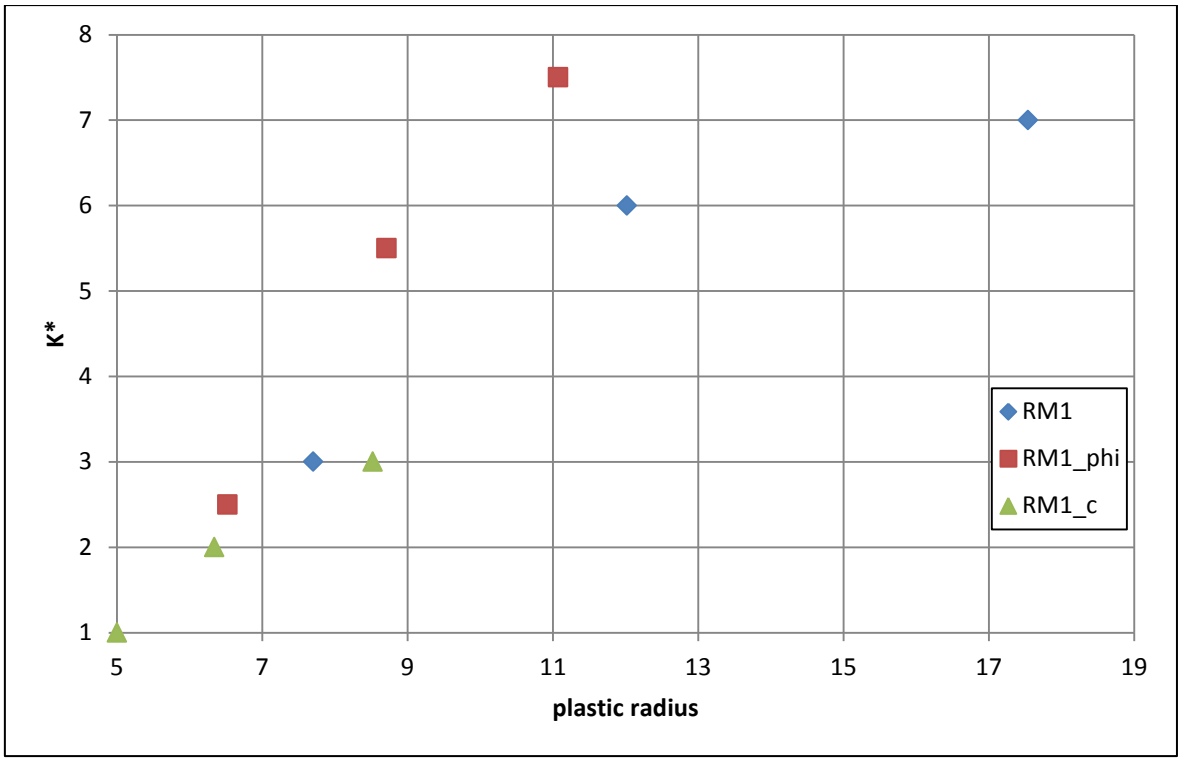

Figure 20: Relationship between plastic radius and the multiplier of the support's effect K*

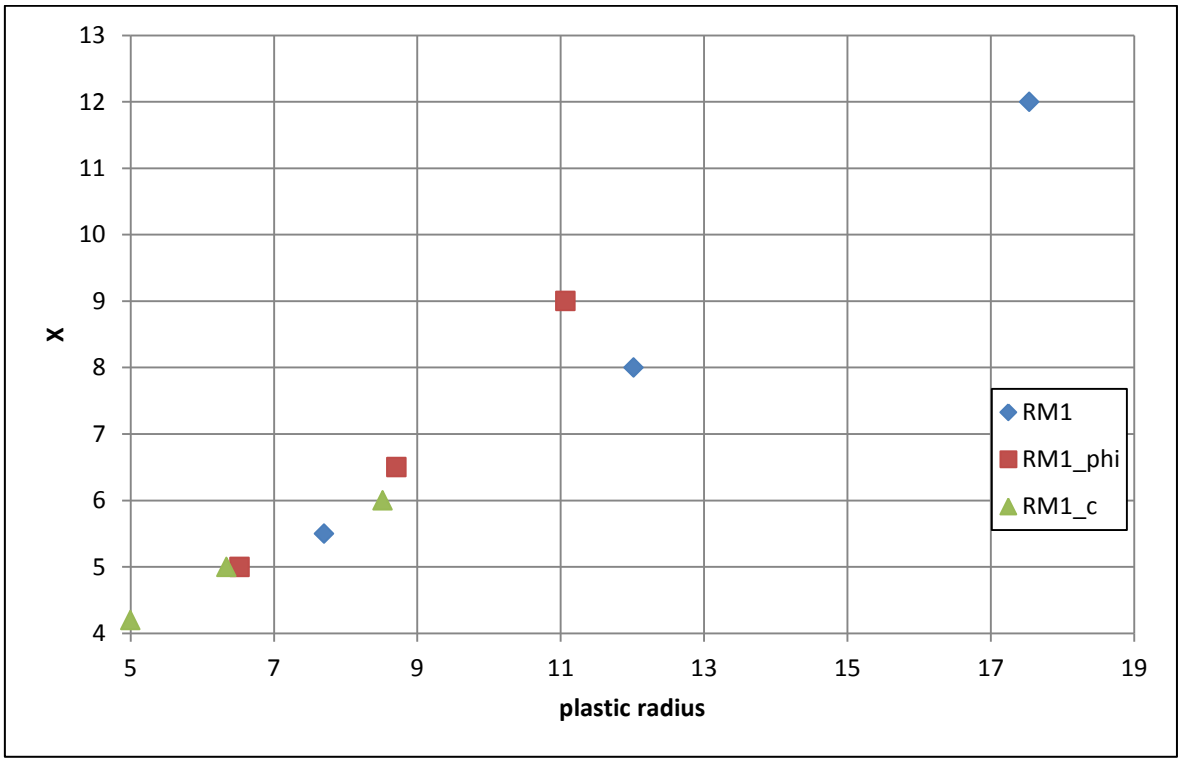

Figure 21: Relationship between plastic radius and curve fitting parameter X

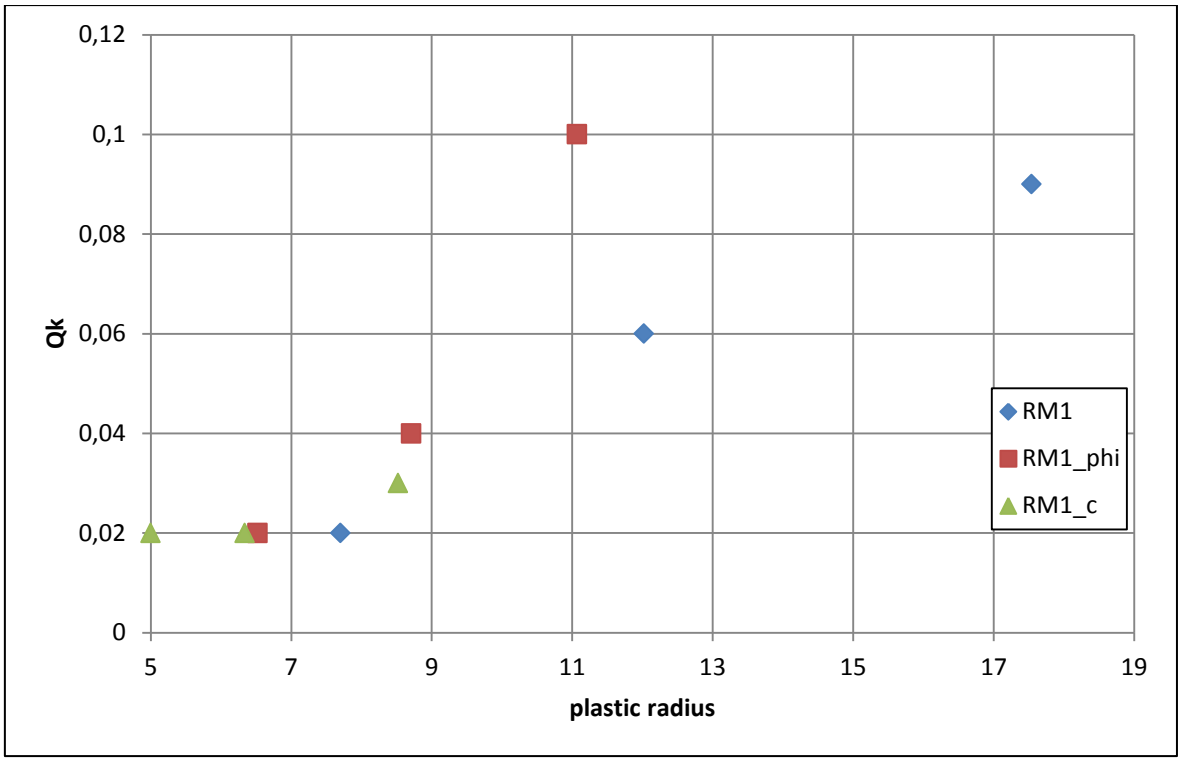

Figure 22: Relationship between plastic radius and the support's influence ahead of its point of installation Q_k

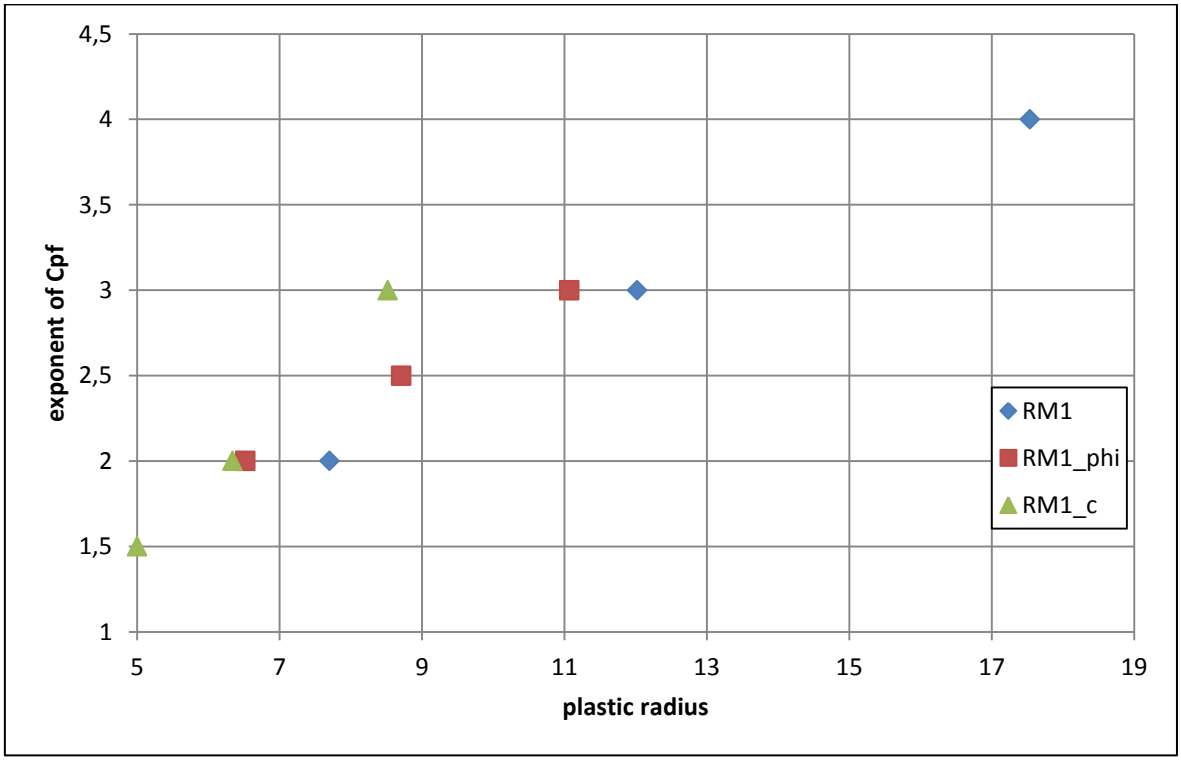

Figure 23: Relationship between plastic radius and the exponent of the time-independent pre-displacement function

These results clearly show that the convergence law, and especially Barlow's extension for the effect of the support, only holds true for elastic conditions. With the proposed value for K by Barlow the decrease in displacements due to the installation of a support system is grossly underestimated for plastic rock mass conditions. Figure 20 shows that the greater the plastic radius is, the bigger the effect of the support is, because more load is transferred from the rock mass to the tunnel lining. But the investigation of rock mass RM1_phi also showed that the plastic radius isn't the only factor governing the support parameter K.

Based on the results of the FLAC^{3D} simulations a function was developed for calculating the K* value. A quadratic function, shown in Eqn. 25, approximates the relationship between plastic radius, initial stress and K* in a proper way.

$$K^* = a + b \cdot \sigma_0 + c \cdot r_{pl} + d \cdot \sigma_0^2 + e \cdot r_{pl}^2 + f \cdot \sigma_0 \cdot r_{pl} \qquad \text{Eqn. 25}$$

where

a = -9.6116
b = -0.6707
c = 2.9968
d = -0.0717
e = -0.2062
f = 0.2097

Figure 24 gives a graphical representation of the quadratic formula for K*. The circles are the values obtained from the numerical analyses. The results from Eqn. 25 should be handled with care and provides a satisfying result only for a limited range of input parameters. For certain parameter combinations the equation results in negative values for K*. A negative K* value would result in a displacement increase due to the installation of a support, which is not realistic.

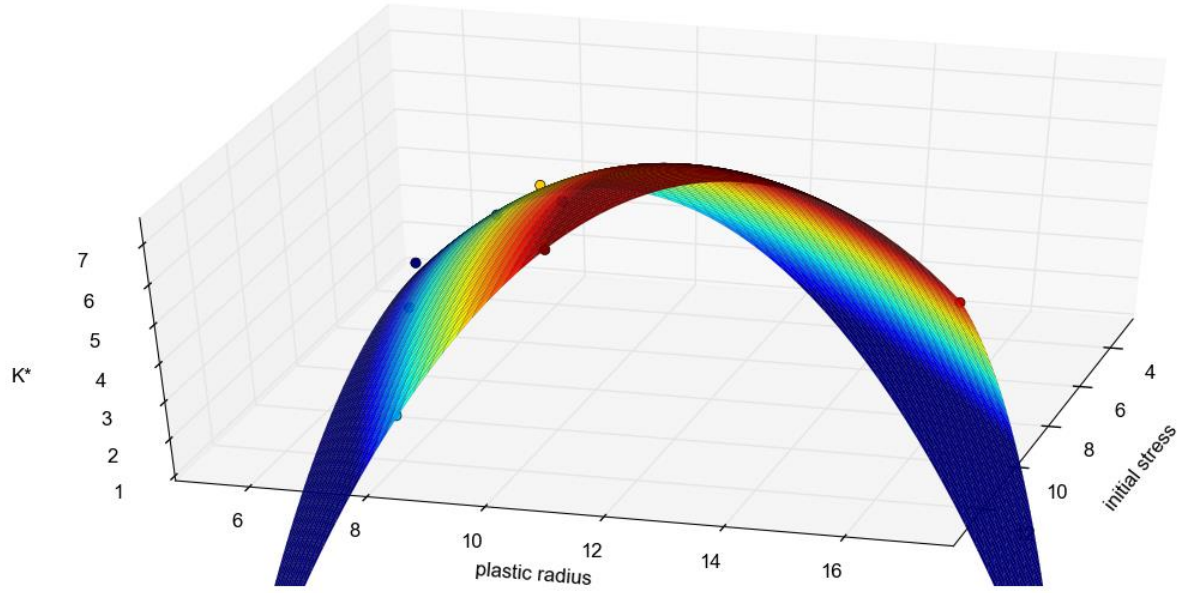

Figure 24: 3D plot of the K* formula

4.3 Shortcomings of the analysis

The above stated investigations do have some drawbacks. Full-face excavation in conventional tunnelling is rather the exception than the rule.
Also the simple constitutive law used for the modelling of the support should be considered as a shortcoming of this analysis. Basically the used material law for the shotcrete has no failure criterion and therefore theoretically allows the tunnel lining to take loading and exhibit displacements up to infinity. Furthermore the time-dependent stiffness development of the shotcrete was neglected and instead a reduced Young's modulus of 4 GPa was used, which is an approximate mean value that should also cover the creep and shrink behaviour of the shotcrete.

Both points mentioned above result in an underestimation of the final displacements and an overestimation of the support capability.

4.4 Sequential excavation analysis

As described in chapter 3.1 calculations using a numerical model with sequential excavation were performed to see if the effect of the support parameter changes significantly compared to the values obtained with the full-face calculations.

The rock mass used was again RM1 (see Table 3) and also the stress states (Table 4) and the support parameters (Table 2) were the same as in the previous numerical simulations. The distance between the top excavation and the bench excavation was set to 10 meters for the first set of calculations. The results of these simulations are listed under the name RM1_10 in Table 8. As it can be seen in Table 8 the results of the full-face excavation and the sequential excavation are almost the same.

Table 8: Comparison full-face excavation and sequential excavation

RM	stress state	C	X	Q_k	K*	exp. of C_{pf}	r_p
RM1	1	-11,3	5,5	0,02	3	2	7,7
	2	-67,46	8	0,06	6	3	12,02
	3	-252,4	12	0,09	7	4	17,54
RM1_10	1	-10, 7	5,5	0,02	2,5	2	7,7
	2	-67,46	8,5	0,06	6	3	12,02
	3	-191	12	0,09	7	4	17,54

To investigate the influence of the distance between the two excavation steps, two more simulations with a distance between the top and the bench of 5 meters (RM1_5) and 20 meters (RM1_20) were carried out. As it can be seen in Table 9 this had almost no influence on the total displacement (as indicated by the factor C) but did change the value of K* slightly.

Table 9: Comparison of the results for different differences between top and bench excavation

RM	stress state	C	X	Q_k	K*	exp. of C_{pf}	r_p
RM1	3	-252,4	12	0,09	7	4	17,54
RM1_5	3	-190,2	10	0,09	5	4	17,54
RM1_10	3	-191	12	0,09	7	4	17,54
RM1_20	3	-192,2	12	0,08	4	4	17,54

Furthermore another calculation was carried out with a slightly different support setup. The shotcrete applied to the top excavation was modified to represent a more realistic behaviour. The first 30 cm of lining above the invert of the top heading were modelled with a shotcrete with a reduced Youngs' modulus to ¼ of the initial value. This resulted in a small reduction of the support parameter K* as can be seen in Table 10. RM1_10_w represents the results obtained from the adjusted shotcrete setup.

Table 10: Comparison of the results for different shotcrete line-up

RM	stress state	C	X	Q_k	K*	exp. of C_{pf}	r_p
RM1	3	-252,4	12	0,09	7	4	17,54
RM1_10	3	-191	12	0,09	7	4	17,54
RM1_10_w	3	-191	12	0,09	6	4	17,54

Overall the sequential excavation analysis showed only a slight decrease of the factor K compared to the values obtained from the full face excavation analysis.

5 Conclusion

The aim of the work was to obtain a better knowledge on the interaction between tunnel and the ground with respect to displacement magnitude and development. The numerical calculations presented in this thesis confirmed that the convergence law proposed by Sulem et al. (1987) and Barlow (1986) provide satisfying results of the displacement development and the effect of the support only for a rock mass with elastic stress-strain behaviour. As soon as plastic deformation occurs in a rock mass, the convergence law differs significantly from the results obtained from the numerical calculations.

With the chosen numerical setup it could be shown, that the size of the plastic radius has a major influence on the convergence law parameters, especially on the influence of the support on the displacement development, represented mainly by the parameter K.

Nonetheless, the results of this thesis do have a limited validity, due to the simplifications in the numerical setup. Further research work is needed to overcome these limitations in order to predict the displacements of a supported tunnel more realistically. A first approach could be the investigation of different lining thicknesses. Since the tunnel lining is modelled as a linear elastic material with no failure criterion and a reduced stiffness, further investigations should focus on an implementation of a more sophisticated constitutive model for the shotcrete.

To further improve results, an aim should also be to represent real excavation scenarios in the numerical model, especially by adjusting the setup for sequential excavation.

References

Barlow, John P. 1986. *Interpretation of Tunnel Convergence Measurements.* The University of Alberta, Canada : Thesis, Department of Civil Engineering, 1986.

Carranza-Torres, C. and Fairhurst, C. 2000. Application of the Convergence.Confinement Method of Tunnel Design to Rock Masses That Satisfy the Hoek-Brown Failure Criterion. *Tunneling and Underground Space Technology.* Vol. 15, 2000, No. 2, pp. 187 - 213.

Feder, G. and Arwanitakis, M. 1976. Zur Gebirgsmechanik ausbruchsnaher Bereiche tiefliegender Hohlraumbauten. *Berg- und Hüttenmännische Monatshefte.* 1976, Vol. 121, 4, pp. 103-117.

Fenner, R. 1938. *Untersuchungen zur Erkenntnis des Gebirgsdruckes.* Essen : Verlag Glückauf GmbH, 1938.

Hoek, E. and Brown, E.T. 1980. *Underground Excavations in Rock.* London : Institute of Mining and Metallurgy, 1980.

Pacher, F. 1964. *Deformationsmessungen im Versuchsstollen als Mittel zur Erforschung des Gebirgsverhaltens und zu Bemessung des Ausbaues.* s.l. : Felsmechanik, 1964.

Panet, M. and Guenot, A. 1982. Analysis of convergence behind the face of a tunnel. *Tunnelling 1982.* The Institution of Mining and Metallurgy, 1982, pp. 197 - 204.

Sellner, Peter J. 2000. *Prediction of Displacements in Tunneling.* Graz University of Technology, Austria : Doctoral Thesis, Institute for Rock Mechanics and Tunnelling, 2000.

Sulem, J., Panet, M. and Guenot, A. 1987. An Analytical Solution for Time-Dependent Displacements in a Circular Tunnel. *Int. J. Rock Mech. Min. Sci. & Geomech. Abstr.* Vol 24, 1987, No. 3.